



Original articles

Research article

<https://doi.org/10.17308/kcmf.2024.26/11936>High-temperature gallium sesquisulfides and a fragment of the T - x diagram of the Ga – S system with these phasesN. Yu. Brezhnev¹, M. V. Dorokhin², A. Yu. Zavrazhnov^{1✉}, N. A. Kolyshkin³, I. N. Nekrylov¹, V. N. Trushin²¹Voronezh State University,
1 Universitetskaya pl., Voronezh 394018, Russian Federation²Physical-Technical Research Institute of UNN (PTRI),
23 Gagarin avenue, BLDG, Nizhny Novgorod 603950, Russian Federation³National Research Center “Kurchatov Institute”,
1 Acad. Kurchatov pl., Moscow 123098, Russian Federation

Abstract

It is known that phases with disordered stoichiometric vacancies are promising candidates for new materials with outstanding thermoelectric, radiation-resistant, catalytic, and other properties, which can be explained by a large concentration of the so-called stoichiometric vacancies, caused by the fact that their stoichiometry does not correspond to the structural type. It is interesting to search for such compounds in A^{III} – B^{VI} semiconductor systems, whose sesquichalcogenides (Me₂Ch₃, Me = Ga, In; Ch = S, Se, Te) are known to have both sphalerite and wurtzite structures and the share of stoichiometric vacancies in the cationic sublattice of about 1/3. The purpose of our study was to determine or confirm the high-temperature structures of gallium sesquisulfides and determine the stability regions corresponding to the phases with these structures on refined T - x diagrams in the high temperature region ($T = 878$ °C).

Various methods of structure and thermal analysis allowed us to prove that at temperatures above 878 °C, close to the stoichiometry of Ga₂S₃, gallium sesquisulfide has four modifications similar in terms of structure, which are connected with each other and other phases of the Ga – S system by enantiotropic transitions. The study confirmed that γ -Ga₂₊₈S₃ with a sphalerite-like cubic structure is formed over a narrow temperature range (878 – 922 °C). The composition of the phase was specified (59.3 mol %). The study demonstrated that at temperatures above 912 °C and a slight excess of gallium (up to ~1 mol %) as compared to the stoichiometry of Ga₂S₃ two modifications are formed: a defected wurtzite-like structure (β -Ga₂S₃, $P6_3mc$) and its derivative phase, whose structure has a lower symmetry (α -Ga₂S₃, $P6_1$) and reaches the stage of congruent melting (1109 ± 2 °C). The study also accounts for the existence of a distectoid transformation α -Ga₂S₃ ↔ β -Ga₂S₃ (~1040 °C). The fourth modification with a monoclinic structure (α' -Ga₂S₃, Cc) is stable over a temperature range from room temperature to ~1006 °C. Its composition satisfies the formula of Ga₂S₃. The article presents a corresponding T - x diagram of the Ga – S system with the areas of existence of the said phases.

Keywords: Ga – S system, Phase diagram, Structure, Stoichiometric vacancies, Vacancy ordering, Synchrotron radiation for the structure analysis

Acknowledgements: *In situ* X-ray powder diffraction studies were performed using the equipment of the National Research Centre “Kurchatov Institute”. The authors are also grateful to A.V. Naumov, Associate Professor at the Department of General and Inorganic Chemistry of VSU, for his participation in discussions.

For citation: Brezhnev N. Y., Dorokhin M. V., Zavrazhnov A. Y., Kolyshkin N. A., Nekrylov I. N., Trushyn V. N. High-temperature gallium sesquisulfides and a fragment of the T - x diagram of the Ga – S system with these phases. *Condensed Matter and Interphases*. 2024;26(2): 225–237. <https://doi.org/10.17308/kcmf.2024.26/11936>

Для цитирования: Брежнев Н. Ю., Дорохин М. В., Завражнов А. Ю., Кольшшин Н. А., Некрылов И. Н., Трушин В. Н. Высокотемпературные сесквисульфиды галлия и фрагмент T - x -диаграммы системы Ga – S с участием этих фаз. *Конденсированные среды и межфазные границы*. 2024;26(2): 225–237. <https://doi.org/10.17308/kcmf.2024.26/11936>

✉ Alexander Y. Zavrazhnov, e-mail: alzavr08@rambler.ru

© Brezhnev N. Y., Dorokhin M. V., Zavrazhnov A. Y., Kolyshkin N. A., Nekrylov I. N., Trushyn V. N., 2024



The content is available under Creative Commons Attribution 4.0 License.

1. Introduction

It is known that when obtaining semiconductor materials, in order to control their properties a lot of attention is paid to the regulation of the concentration of point defects, including *vacancies*. However, structures of some of the promising semiconductors demonstrate disorder in one or several sublattices due to the fact that the stoichiometry of the materials does not correspond to the structural type. As a result, the occupancy of certain sites in one or several sublattices is significantly lower than 100%. In a number of compounds, such unoccupied vacancies, called *stoichiometric vacancies*, can have great concentrations, up to tens of mol % [1]. Since *stoichiometric vacancies* are essential structural elements, they cannot be strictly classified as point defects. However, several terms can be found in the literature on the problem, including defect structures and defect sphalerite (wurtzite, spinel) structures.

Structures with stoichiometric vacancies result in unique properties, which are not observed in compounds with classical vacancies*. These properties include good thermoelectric properties, high radiation resistance, a wide variety of lattice parameters in films, etc. [1–6].

In our study, we focused on the samples of such substances in the Ga – S system, which is one of the least studied among the $A(III) - B(VI)$ systems. It is known that gallium sulfides with stoichiometry close to Ga_2S_3 crystallize in sphalerite- and wurtzite-like structures with stoichiometric vacancies in the cationic sublattice ($\sim 1/3$ of the number of nodes) [7]. Detailed in the literature are a large variety of phases formed as a result of the ordered and disordered arrangement of these vacancies. However, little is known about the conditions for obtaining gallium sesquisulfides with a particular structure. Recent studies [8–10] demonstrated that besides the α' - Ga_2S_3 phase (one of the derivatives of the defect wurtzite with ordered vacancies), which is stable over a wide temperature range, there is another compound – γ - $Ga_{2+\delta}S_3$, which has a sphalerite-like cubic structure with disordered vacancies. This

modification is stable over a narrow temperature range as compared to other phases (from 878 to 922 °C) and is shifted towards a significant excess of gallium (0.5 mol %). At the same time, [9, 10] as earlier [11, 12] reported the presence of other gallium sesquisulfides on the phase diagram, whose regions of existence correspond to even higher temperatures than those of γ - $Ga_{2+\delta}S_3$.

The purpose of our study was to determine or confirm the structures of gallium sesquisulfides and determine the stability regions corresponding to the phases with these structures on refined T - x diagrams in the high temperature region ($T \geq 878$ °C).

2. Experimental

The study was divided into several stages. During the preliminary stage, we obtained gallium sulfide alloys with various concentrations of components using the method of direct two-temperature synthesis described in [8]. The compositions of the alloys (1–2 g) used in structural studies corresponded to the concentration range of 58.0–60.2 mol % with the concentration of sulfur in the samples changing at an interval of 0.1–0.2 mol %. Ampoules with the obtained ingots were annealed for 24 hours at temperatures from 900 to 1080 °C, after which they were quenched in iced water. The samples were then taken out of the ampoules and ground to powder.

During the first stage of the experiment, we conducted powder diffraction of the obtained alloys. Some of the samples were studied *in situ* under equilibrium conditions at high temperatures using synchrotron radiation. However, most of the powder diffraction patterns were obtained for quenched samples at room temperature.

During the second stage, we performed a differential thermal analysis of each of the samples and an analysis of the alloys with a wider concentration range: from 50.0 to 60.7 mol %. In our experiments, we used the methodology presented in [8, 13]. During the final stage, we compared the results obtained by means of different methods.

The synchrotron radiation experiments were conducted at the National Research Centre “Kurchatov Institute” on the Structural Materials

* Classical vacancies can be explained by deviations of the composition of the solid phase from the ideal stoichiometry and disordering of the crystal structure at higher temperatures.

Science station of Kurchatov Synchrotron Radiation Source, channel K1.3b. The powder of the studied compound was put into a quartz-glass capillary with a diameter of 0.3–0.7 mm and a length of 25–30 mm. The vacuumed and sealed capillary was then put into a resistance heating furnace with a narrow X-Ray entrance slit. A chromel-alumel thermocouple was placed in 1–3 mm from the capillary. A *Dectris Pilatus 300K-W* detector was placed about 20 cm behind the sample (the distance was determined based on the diffraction data for the studied sample obtained at room temperature). The furnace heated to high temperatures (860 °C) in about 5 hours. The criterion used to estimate the time required to reach the equilibrium was the complete identity of the diffraction patterns obtained while increasing and decreasing the temperature step by step. The time required to obtain each diffraction pattern was ~ 0.5 hour.

The method was chosen due to the fact that a noticeable pressure of chemically aggressive vapors (Ga_2S , S_2) over gallium sulfides prevented us from using the equipment traditionally used in *HT-XRD* experiments. The walls of the capillary with a thickness of ~10 μm are almost transparent for synchrotron radiation with a photon energy of 18055 eV (at a wavelength of 0.6867 Å). They absorb less than 2% of the energy. Together with the high energies of synchrotron radiation this allowed us to register the diffraction pattern of the powder in the capillary. The upper temperature limit was 1015 °C, which was only due to the characteristics of the heating element.

The X-ray crystallography of the annealed and quenched samples was performed at room temperature using an *Empyrean B.V.* diffractometer ($\text{CuK}_{\alpha 1}$ -radiation in the 2θ range from 10° to 95°, step 0.02°, the exposure time at each point at least 0.2 s).

To analyze the data, we modelled calculated diffraction patterns of the powder based on the literature data using the *PowderCell 2.4* software package [14]. The experimental diffraction patterns obtained on the Kurchatov Synchrotron Radiation Source were integrated in the *Fit2D* software [15], which was also used to calibrate the distance between the sample and the detector. The results were presented in terms of the

$\text{CuK}_{\alpha 1}$ -radiation (1.54060 Å). The *Unitcell* software was used for the refinement of cell parameters [16]. The reflections observed on the diffraction patterns were identified by means of comparison with the literature data [10].

The differential thermal analysis (DTA) was conducted on a unit consisting of TPM-101 and TPM-200 sensor units and temperature sensors in the form of chromel-alumel and nichrosil-nisil thermocouples. The averaged signal being transmitted to the computer every second. The quantitative data was obtained using heating mode only with heating rates from 0.9 to 4.0 K/min. Relatively low heating rates were used to differentiate between phase transformations occurring at similar temperatures and to prevent the emergence of metastable states. Inaccuracies in the temperatures of phase transformations on the horizontal lines of the T - x diagram were determined based on the statistical processing of all temperatures obtained for a particular horizontal for different compounds. The smallest possible inaccuracy was assumed to be ± 2 °C, which is a standard inaccuracy for chromel-alumel and nichrosil-nisil thermocouples. If the value obtained after statistical processing was lower, the final accuracy was still ± 2 °C.

The analysis of the DTA data allowed us to determine the inaccuracy in the composition of the samples. Alloys with compositions differing by 0.1 mol % demonstrated reproducibly different effects. For instance, the horizontal line at 910 °C – eutectic melting of $\text{GaS} + \gamma\text{-Ga}_{2+8}\text{S}_5 \rightarrow \text{L}$ – was observed in samples with a concentration of sulfur of up to 59.2 mol %. However, it was not observed for the alloy with $x_s = 59.3$ mol %. Therefore, we assumed that the concentration inaccuracy in the samples was close to ± 0.1 mol %.

The compositions of phases participating in non-variant equilibria were refined when comparing the peak areas on the DTA thermograms. It is obvious, that these areas are proportional to the molar heat of phase transformations. Then, when studying the disproportionation of the condensed phase Φ_2 into two other condensed phases (which occurs, for instance, during incongruent melting):



or the comproportionation of Φ_1 and Φ_3 into Φ_2 (a reaction is reverse to (1): for instance, eutectic melting) the absorption of heat by the sample is maximum, if the bulk composition of the studied compound coincides with the composition of the Φ_2 phase. This composition corresponds to the maximum peak area on the DTA thermogram*.

Since it is extremely difficult to conduct thermographic experiments with identical amounts of substances, it is practical to analyze normalized areas (S^*) rather than absolute areas (S), where in formula (2) n is the amount of substance in a Stepanov ampoule:

$$S^* = \frac{S}{n}. \quad (2)$$

We should note that dependences $S^* = f(x_s)$ are constructed according to the Tamman's method and consequently look similar to the Tamman's triangle [17].

3. Results

Monoclinic α' -Ga₂S₃ and cubic sphalerite-like γ -Ga_{2+ δ} S₃ modifications. The results of the powder diffraction analysis of the alloys of various compositions annealed at different temperatures (and quenched at these temperatures) are given in Figs. 1 and 2 and table 1. Fig. 1 demonstrates typical diffraction patterns, which vary depending on the annealing temperature and the composition of the alloy. The diffraction patterns close to curve 1 with a large number of diffraction maxima were observed for all the annealed samples in the studied concentration range (58.0–60.2 mol %), if the annealing temperatures were below 870 °C. The same diffraction patterns were observed for all the alloys which, instead of quenching, were slowly cooled to room temperature in the switched-off furnace. A full-profile analysis of the diffraction patterns demonstrated that the main phase in such samples was the monoclinic modification of α' -Ga₂S₃. When the concentration of sulfur was from 59.8 to 60.2 mol %, this modification was the only one. At lower concentrations of chalcogen (58.0–59.6 mol %) an impurity phase appeared –

gallium monosulfide (a hexagonal modification of GaS-2H, $P6_3mmc$).

At higher annealing temperatures (905 and 910 °C) alloys with an excess of gallium in relation to the stoichiometry of Ga₂S₃ (the concentration of sulfur from 58.0 to 59.8 mol %) demonstrated rare wide maxima of a specific form, (curve 2, Fig. 1). Taking into account the data of transmission electron microscopy [10], these maxima indicated the presence of a sphalerite-like cubic structure γ -Ga_{2+ δ} S₃ with disordered stoichiometric vacancies. However, this did not happen in the alloys with the maximum concentration of sulfur (from 59.8 to 60.2 mol %), and monoclinic modification of α' -Ga₂S₃ remained at least up to 1000 °C.

The results of the high-temperature X-ray phase analysis of the alloy with the concentration of sulfur of 58.0 mol % conducted using synchrotron radiation (curve 2, Fig. 1) were thoroughly analyzed. They demonstrated that the cubic modification of γ -Ga_{2+ δ} S₃ can be stable as compared to other phases under equilibrium (it does not occur as a result of quenching and decomposition of other structures). For this composition, at temperatures 883, 893, and 903 °C γ -Ga_{2+ δ} S₃ coexisted with gallium monosulfide GaS. When the sample was kept at 918 °C, the diffraction maxima of GaS disappeared and the diffraction pattern demonstrated a wide halo together with rare peaks of the γ -phase. This indicates the formation of a sulfide melt as the second (impurity) phase. It should be noted that [10] describes the results of a similar study of this alloy. However, it only focused on the equilibrium at a single temperature (918 °C).

Hexagonal high-temperature phases: wurtzite-like β -Ga₂S₃ ($P6_3mc$) and its derivative α -Ga₂S₃ ($P6_1$). [10] proved that at temperatures above 922 °C the sphalerite-like γ -Ga_{2+ δ} S₃ undergoes peritectic decomposition into a melt and another high-temperature phase \sim Ga₂S₃. However, the analysis of the structure of the substance obtained after quenching at $T \geq 945$ °C always demonstrated a mixture of hexagonal phases (α -Ga₂S₃, β -Ga₂S₃, and – for some samples – GaS).

In our study, we maintained the annealing temperature (from 940 to 1080 °C) of vacuumed quartz ampoules with ground alloys of various compositions close to Ga₂S₃ for a long time

* This is true, if we compare the results of DTA conducted using identical number of compounds with the same thermal conductivity and heat loss values. At the same time, changes in the quantity of the vapour phase equilibrium with Φ_1 , Φ_2 , and Φ_3 should be negligibly small.

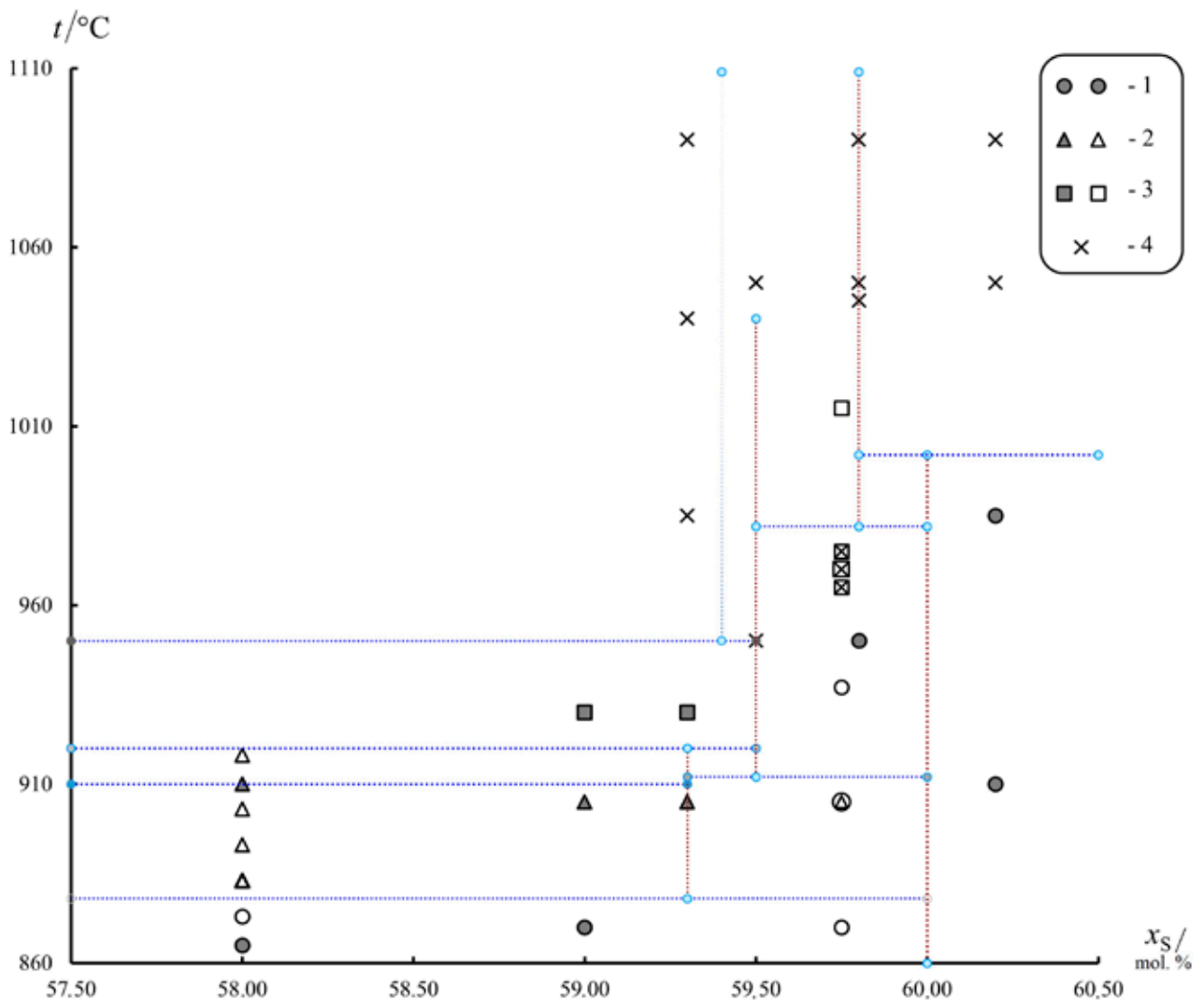


Fig. 2. Compositions of samples of the Ga – S system identified during X-ray powder analysis versus the T - x -coordinates of the phase diagram. **Notation.** Annealed and quenched alloys are designated as dark, gray-filled figures – circles, triangles, squares, crosses; the samples, which studied *in situ* at high temperatures in a “synchrotron” experiment are designated as light figures without shading. Digital designations: 1 – α' - Ga_2S_3 (+ traces of GaS for samples with $x_S < 60.0$ mol %), 2 – γ - $\text{Ga}_{2+\delta}\text{S}_3$ (+ traces of GaS for temperatures less than 910 °C), 3 – β - Ga_2S_3 , 4 – α - Ga_2S_3 . The dotted lines indicate the horizontals obtained from the DTA results; the compositions of the probable phases are marked as vertical dotted lines

in quenched samples over all the studied concentration range, up to the sample with the concentration of sulfur of 60.2 mol %. In all the experiments, phase α - Ga_2S_3 was identified as the only one (curve 4, Fig. 1). The monoclinic modification α' - Ga_2S_3 , which is the most stable at room temperature, was not registered even as an impurity phase and even in the samples with the highest concentration of sulfur (60.2 mol %).

The differential thermal analysis (DTA) allowed us to obtain an approximate T - x diagram

of the Ga – S system. However, before we present the diagram, we should point out several characteristic features registered on differential heating curves for the alloys of Ga – S of various compositions.

56.0–59.0 mol % region. For the samples corresponding to this concentration interval, thermograms were registered, which, besides the minimum associated with the liquidus line, demonstrated deep endoeffects at temperatures of 878, 910, and 922 °C (Fig. 4a).

Table 1. Thermal stability of the condensed phases for the Ga – S system and the structures of these phases

Фаза	Lower temperature limit of the phase stability and the correspondent phase equilibrium	Upper temperature limit of the phase stability and the correspondent phase equilibrium	Structure, cell parameters and the presence of ordered (+) or disordered (-) vacancies	Состав твердой фазы, мол. % S
$\gamma\text{-Ga}_{2+\delta}\text{S}_3$	$878 \pm 2 \text{ }^\circ\text{C}$, $\text{GaS} + \alpha'\text{-Ga}_2\text{S}_3 = \gamma\text{-Ga}_{2+\delta}\text{S}_3$ (I) , eutectoid	$922 \pm 4 \text{ }^\circ\text{C}$, $\gamma\text{-Ga}_{2+\delta}\text{S}_3 = \beta\text{-Ga}_2\text{S}_3 + \text{L}$ (II) peritectic	cubic, sphalerite-like, S.G. $F\bar{4}3m$, $a = 5.17 - 5.21 \text{ \AA}$, (-)	59.3
L расплав	$910 \pm 3 \text{ }^\circ\text{C}$ $\text{GaS} + \gamma\text{-Ga}_2\text{S}_3 = \text{L}$ (III) eutectic	–	melt of gallium sulfides	–
$\beta\text{-Ga}_2\text{S}_3$	$912 \pm 3 \text{ }^\circ\text{C}$, $\gamma\text{-Ga}_{2+\delta}\text{S}_3 + \alpha'\text{-Ga}_2\text{S}_3 = \beta\text{-Ga}_2\text{S}_3$ (IV) eutectoid	$\sim 1040 \text{ }^\circ\text{C}$, $\beta\text{-Ga}_2\text{S}_3 = \alpha\text{-Ga}_2\text{S}_3$ (V) distectoid	Hexagonal, wurzite-like, S.G. $P6_3mc$, $a = 3.682$, $b = 6.031 \text{ \AA}$, (-)	59.8
$\alpha\text{-Ga}_2\text{S}_3$	$\sim 950 \text{ }^\circ\text{C}$ (from the Ga-side), $\text{L} + \beta\text{-Ga}_2\text{S}_3 = \alpha\text{-Ga}_2\text{S}_3$ (VI) cathatectic $\sim 982 \text{ }^\circ\text{C}$ (from the S-side), $\beta\text{-Ga}_2\text{S}_3 + \alpha'\text{-Ga}_2\text{S}_3 = \alpha\text{-Ga}_2\text{S}_3$ (VII) eutectoid	$1109 \pm 2 \text{ }^\circ\text{C}$, $\alpha\text{-Ga}_2\text{S}_3 = \text{L}$ (VIII) Congruent melting	hexagonal, S.G. $P6_1$, $a = 6.3883$, $b = 18.081 \text{ \AA}$, (+)	59.0–60.2
$\alpha'\text{-Ga}_2\text{S}_3$	Stable at RT	$1002 \pm 2 \text{ }^\circ\text{C}$, $\alpha'\text{-Ga}_2\text{S}_3 = \text{L} + \alpha\text{-Ga}_2\text{S}_3$ (IX) peritectic melting	моноклинная, ПГ Cc , $a = 11.14$, $b = 6.41$, $c = 7.04 \text{ \AA}$, $b = 121.2^\circ$, (+)	60.0
GaS-(2H)	Stable at RT	$967 \pm 2 \text{ }^\circ\text{C}$ [10], $\text{GaS} = \text{L}$ (XI) congruent melting	Layered hexagonal, S.G. $P6_3mmc$, $a = 3.59$, $b = 15.43 \text{ \AA}$ [10]	50.0

The results of the detailed* differential thermal analysis (DTA) confirm the results of the structure analysis, which indicated the stability of the $\gamma\text{-Ga}_{2+\delta}\text{S}_3$ phase over a small range of temperatures and compositions. Furthermore, the results of the DTA allowed us to specify this range. Taking into account the results of the structure analysis, the first effect demonstrates that the lower limit of the temperature range is the eutectoid decomposition into GaS and monoclinic $\alpha'\text{-Ga}_2\text{S}_3$ ($878 \pm 2 \text{ }^\circ\text{C}$; equation **(I)**, Table 1). The latter effect indicates the upper limit of the γ phase. It is associated with incongruent melting, which, besides the melt, results in the formation of another high-temperature modification Ga_2S_3 ($922 \pm 2 \text{ }^\circ\text{C}$; equation **(II)**, Table 1). Finally, the intermediate effect ($910 \text{ }^\circ\text{C}$) is associated with eutectic melting (equation **(III)**, Table 1).

* The study included 75 samples. Each sample was analysed at three heating rates: 0.9, 1.9, and 3.8 K/min.

The analysis of the dependences of normalized areas of endoeffects on thermograms allowed us to specify the composition of the $\gamma\text{-Ga}_{2+\delta}\text{S}_3$ phase at the lower and the upper limits of existence of the phase on the *T-x* diagram. According to Fig. 3, the lower limit corresponds to the concentration of sulfur of $59.3 \pm 0.1 \text{ mol } \%$. A similar value was obtained for the upper limit of existence of this modification, which is 0.2 % less than stated in [10].

59.0–59.5 mol % region. In this concentration range, all the above mentioned peaks, except for the last one ($910 \text{ }^\circ\text{C}$), were also quite prominent, which indicated that the compositions were close to the region of existence of $\gamma\text{-Ga}_2\text{S}_3$.

59.5–59.8 mol % region. In this region, there was a decrease in the temperature of the effect (which was previously registered at $922 \text{ }^\circ\text{C}$) to $916\text{--}917 \text{ }^\circ\text{C}$. This indicated a change in the nature of the effect. Taking into account the X-ray data, the corresponding transformation

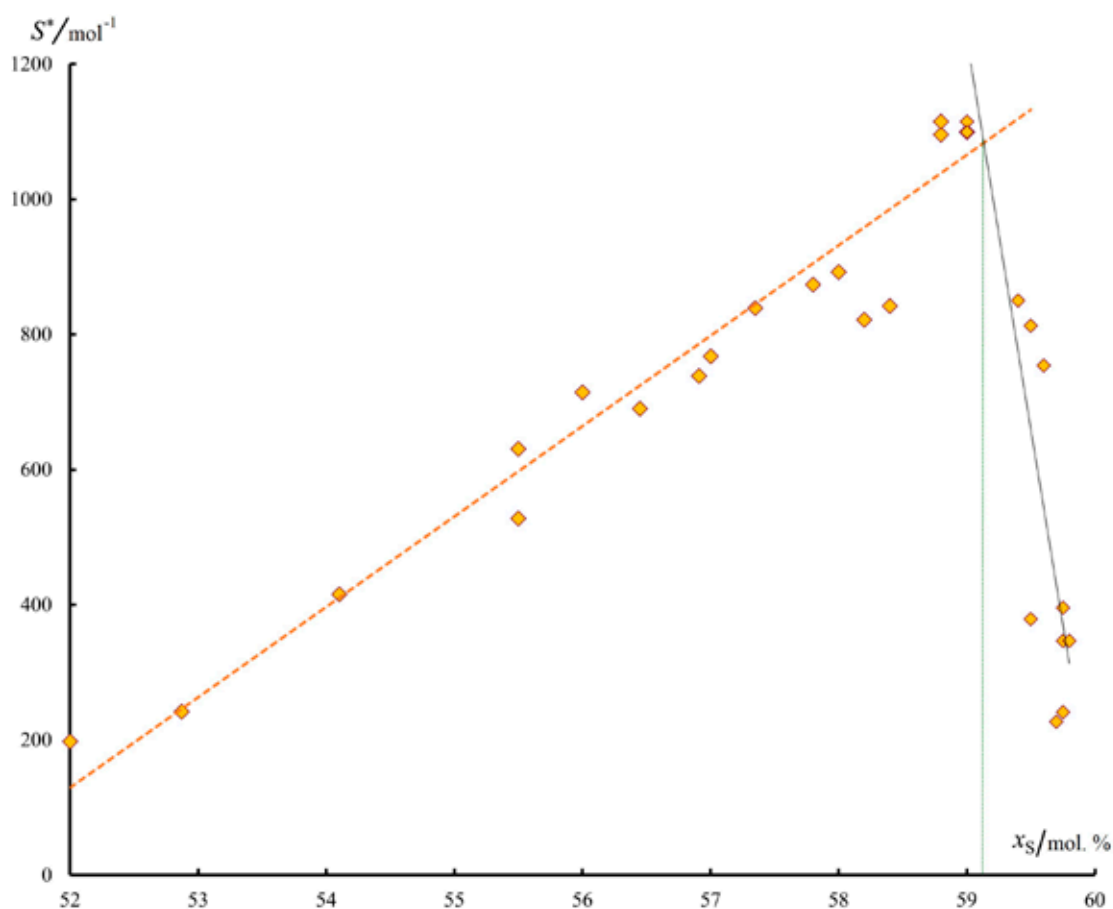


Fig. 3. The dependence of the reduced peak area on the alloy compositions for the DTA heating patterns, focused on the endo-effect observed at a temperature of ~ 878 °C

is associated with the formation of a new phase β - Ga_2S_3 from γ - $\text{Ga}_{2+\delta}\text{S}_3$ and α' - Ga_2S_3 according to the reaction reverse to eutectoid transformation – see equation (IV), Table 1.

The 59.8 mol % composition demonstrated a slight effect at 1040 °C (Fig. 4b), which can indicate the decomposition of the phase and which we classified as a distectoid transformation – equation (V), Table 1. Furthermore, at a temperature of 955–960 °C an additional endoeffect appeared (Fig. 4b), whose area increased at higher concentrations of sulfur in the studied samples. Taking into account the results of powder diffraction, we associated this effect with the formation of the α - Ga_2S_3 phase from the melt and β - Ga_2S_3 according to the catatectic reaction (see equation (VI), Table 1).

59.9 mol % composition. This composition is interesting because all the above mentioned effects (878, 917, and 950 °C) disappear from the thermogram, while a new one appears and is reproduced at a temperature of ~ 982 °C. We

interpreted this effect as satisfying equation (VII), Table 1.

60.0–60.7 mol %s region. All the thermal experiments conducted in this region demonstrated the presence of a strong effect at 1002 ± 2 °C, which is most probably associated with the peritectic decomposition of the α' - Ga_2S_3 phase (equation (IX), Table 1).

For the alloy with the concentration of sulfur of 60.0 mol %, the maximum liquidus temperature is reached and the form of the effect becomes typical for the phase transformation of the I kind. This indicates congruent melting of the α - Ga_2S_3 phase (1109 ± 2 °C).

The results of the DTA (Table 1) together with the results of powder diffraction (Fig. 2) allowed us to obtain a fragment of the T - x diagram of the Ga – S system refined for the concentration range from 50.0 to 60.7 mol %. The diagram is presented in Fig. 5.

Metastable states in the Ga – S system. As we have previously mentioned, three out

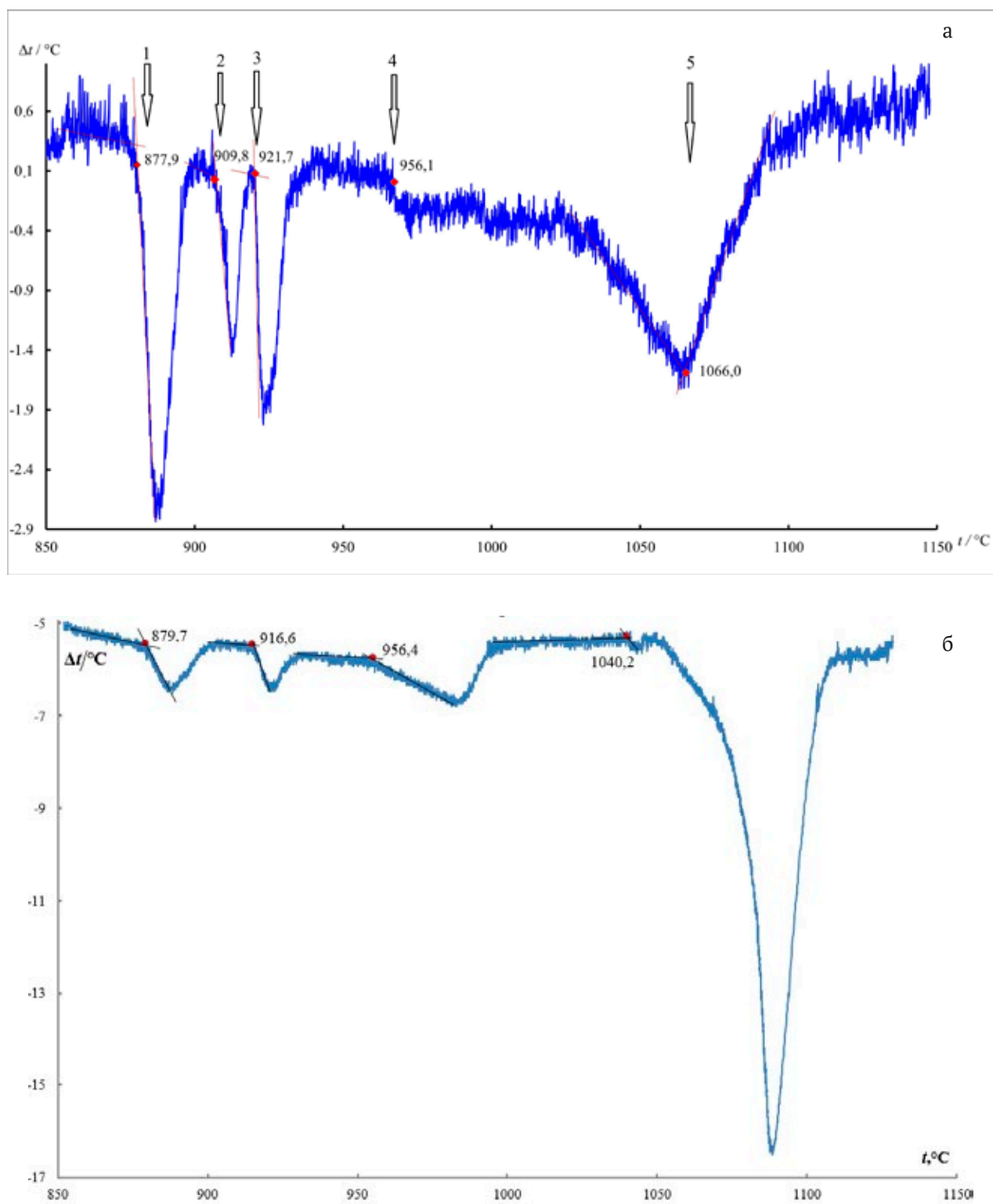


Fig. 4. DTA heating patterns of the Ga – S alloys with a sulfur content of 58.8 (a) and 59.8 (b) mol % S at rates of 2 and 4 K/min, respectively

of four phases of the Ga_2S_3 family (α , β , and γ - $\text{Ga}_{2+\delta}\text{S}_3$) are metastable at room temperature and can be obtained only through quenching at high temperatures at which they are stable as compared to other phases. In order to determine the conditions under which these phases transform into their stable modifications at noticeable rates, samples of phases α -, β -, and γ (with the concentration of sulfur of 59.8 mol % for the first two phases and 59.3 mol % for the third phase) were studied in DTA experiments, where they were heated starting with room temperature at a heating rate of ~ 2 K/min. Thermograms of all the samples demonstrated noticeable exoeffects: β - Ga_2S_3 sulfide (460 ± 10 °C) was the most susceptible to decomposition; modifications γ - $\text{Ga}_{2+\delta}\text{S}_3$ and α - $\text{Ga}_{2+\delta}\text{S}_3$ also demonstrated exoeffects close to 700 and 650 °C respectively. In all the cases, the result of the transformation was a monoclinic modification α' - Ga_2S_3 (with an impurity of GaS). In order to determine the heat of the phase transition



a sample of the β modification was analyzed using a *Hitachi DSC 7020* differential scanning calorim-

eter over a temperature range from 25 to 600 °C in a highly pure (99.999 %) nitrogen atmosphere. The heat of the phase transformation calculated based on the peak area was 15.9 J/g, which corresponds to 3.75 kJ/mol in relation to the idealized stoichiometry of Ga_2S_3 . Unfortunately, it was impossible to estimate the thermal effects of the relaxation of two other high-temperature phases in the α' phase due to the temperature limitations (~ 600 °C) of the equipment.

During the DTA of the studied phase transformations observed during slow (2–4 K/min) cooling of the samples at temperatures outside the stability regions of high-temperature phases, the cooling curves demonstrated the same main effects as the heating curves. However, these effects correspond to significantly lower temperatures. Thus, the most high-temperature modification α - Ga_2S_3 , which was in contact with melt L, (compositions from 58.0 to 59.5 mol %) is supercooled to a temperature of ~ 890 °C, below which it transforms into γ - $\text{Ga}_{2+\delta}\text{S}_3$. In turn, γ - $\text{Ga}_{2+\delta}\text{S}_3$ when slowly cooled decomposes into GaS and α' - Ga_2S_3 only at 830–840 °C, i.e. It endures long-term supercooling up to almost 50 °C as compared to the lowest temperature of its

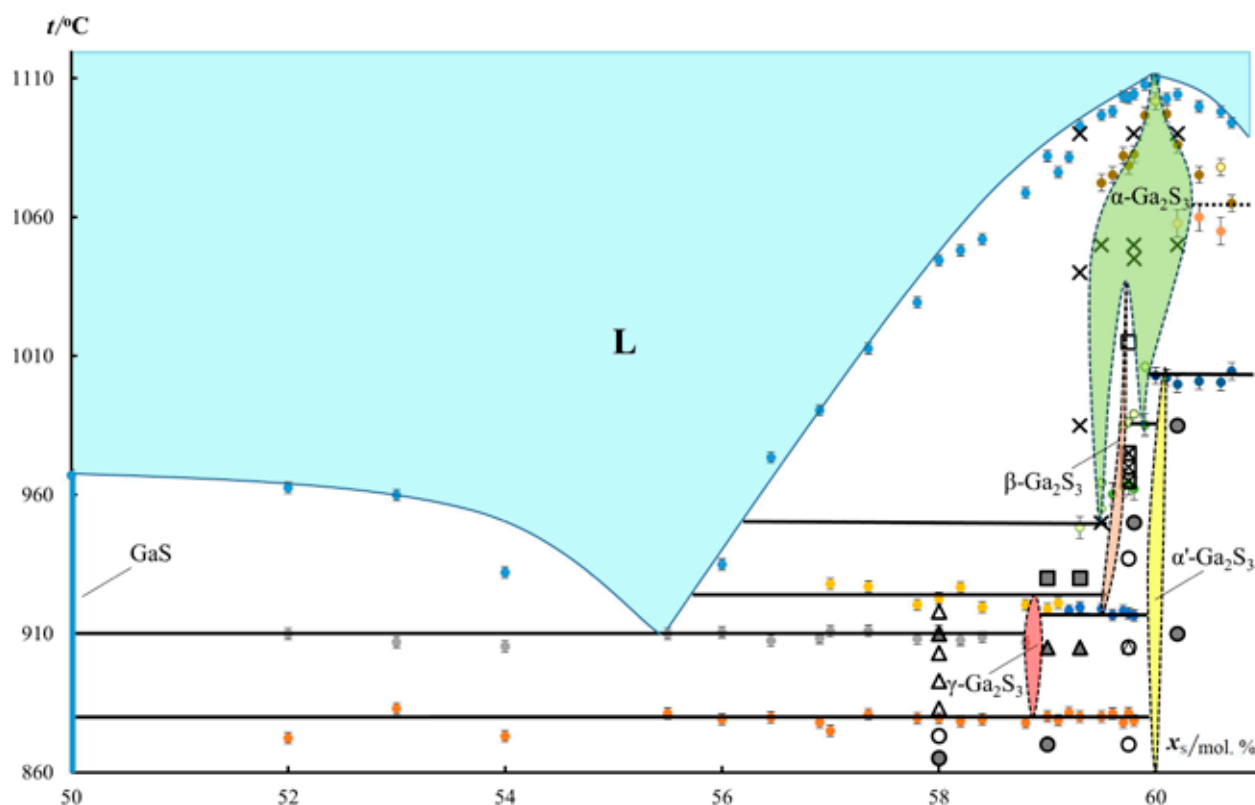


Fig. 5. Fragment of the T - x -diagram for the Ga – S system according to the data of this work

stability region. Other horizontal lines also shift noticeably towards lower temperatures. Thus, the eutectic horizontal satisfying the reaction reverse to (III) (Table 1) shifts by ~ 15 °C from its position on the T - x diagram, and the temperature of peritectic crystallization of α' - Ga_2S_3 (reaction opposite to (IX), Table 1) shifts by ~ 25 °C. Other peculiarities are that in cooling modes *a*) there were no transformations indicating the formation of the β - Ga_2S_3 phase and *b*) congruent crystallization of gallium sesquisulfide (α - Ga_2S_3) proceeded almost without supercooling.

4. Discussion

A shift of the regions of existence of defect phases towards the excess of the cation former (Ga, In). Let's consider the fact that the regions of existence of all sesquisulfides from the Ga_2S_3 family are shifted towards an excess of the cation former (Ga). The only exception is the α' - Ga_2S_3 phase whose composition corresponds to the ideal stoichiometry (60.0 mol %) within an inaccuracy of 0.1 mol %.

Here we can use the concept of *valence electron concentration* [18, 19], according to which structures with bonding networks close to the structure of diamond can be formed at a valence electron concentration (*VEC*) from 4.00 to 4.80 (in certain cases up to 4.92). *VEC* is defined as the number of valence electrons per formula unit. Despite being rather formal, this approach can be effective when predicting the stoichiometry of some solid-phase compounds. In particular, it explains a noticeable shift of the composition of the cubic γ phase $\text{Ga}_{2+\delta}\text{S}_3$ towards an excess of gallium as compared to the ideal stoichiometry of Ga_2S_3 . Thus, with the concentration of sulfur in the phase being 59.3 mol %, we obtain $\delta = 0.06$ and *VEC*:

$$VEC = \frac{2.06 \cdot 3 + 3 \cdot 6}{(2.06 + 3)} = 4.77. \quad (5.1)$$

The actual *VEC* can be even smaller (by several hundredths) than the calculated value 4.77, because the electrons of the gallium atoms that partially occupy the vacancies in the cationic sublattice of the cubic $\text{Ga}_{2+\delta}\text{S}_3$ phase may have little impact on the formation of the chemical bond. We should note that a small shift of the composition of the γ phase towards gallium as

compared to the ideal composition of Ga_2S_3 , for which *VEC* would be almost 4.80, is in good agreement with the fact that the valence electron concentration in the structure tends to decrease. However, even after this shift *VEC* ≈ 4.7 is still close to the upper stability limit, which makes the $\text{Ga}_{2+\delta}\text{S}_3$ phase metastable outside the narrow region of temperatures and compositions.

Taking into account the closeness of the bonding networks in wurtzite- and sphalerite-like structures, it is also logical that the homogeneity ranges of both wurtzite-like β - Ga_2S_3 and its modification α - Ga_2S_3 shift towards gallium. It also explains the fact that these phases are only stable over a limited temperature range.

Thermal stability. Wurtzite-like modifications can exist at higher temperatures than sphalerite-like structures, which is common for many binary phases, for instance, ZnS [20]. It is logical that the homogeneity ranges of the phases based on a “defect” wurtzite β - and α - Ga_2S_3 are generally located on the T - x diagram of the Ga – S system above the region of existence of the *sphalerite-like* modification γ - $\text{Ga}_{2+\delta}\text{S}_3$.

Characteristics that require further analysis. As quite unexpected came the fact that a more ordered phase β - Ga_2S_3 has a narrow homogeneity range, while its superstructural modification α - Ga_2S_3 with ordered vacancies has a wider homogeneity range and can be formed at higher temperatures than the β phase. This fact requires further analysis. At the same time, the vacancies of the α - Ga_2S_3 phase are only relatively ordered. This structure demonstrates crystallographically different positions of gallium in the cationic sublattice, which changes the symmetry and induces the transition $P6_3mc \rightarrow P6_1$. Different cationic positions in the α - Ga_2S_3 structure are partially occupied to different degrees. However, they remain disordered, because partial occupation is stochastic. On the contrary, stoichiometric vacancies of another modification of the wurtzite-like structure of the β phase, a monoclinic α' - Ga_2S_3 , are almost completely ordered. As a result, this phase is significantly different in terms of stability from the disordered and partially ordered modifications: α' - Ga_2S_3 is almost completely stoichiometric and stable over a wide range of temperatures, starting from room temperature.

Although some of the results of the study require further research, we can conclude that the results are relevant, because they were obtained using various methods and are in good agreement with each other.

5. Conclusions

Using several independent methods of structure analysis (X-ray powder diffraction and high-temperature diffraction by means of synchrotron radiation), we confirmed that the high-temperature phase found during electron-diffraction studies (TEM, DAED) and formed at temperatures from 878 to 922 °C has a cubic sphalerite-like structure $F\bar{4}3m$ with disordered stoichiometric vacancies. The composition of the phase further referred to as $\gamma\text{-Ga}_{2+\delta}\text{S}_3$ was specified ($\delta \approx 0.06$ or $x_s = 59.3$ mol %). The study demonstrated that at temperatures above 912 °C and a slight excess of gallium (up to ~1 mol %) as compared to the stoichiometry of Ga_2S_3 two modifications are formed: a defected wurtzite-like structure ($\beta\text{-Ga}_2\text{S}_3$, $P6_3mc$) and its derivative phase, the structure of which has lower symmetry ($\alpha\text{-Ga}_2\text{S}_3$, $P6_1$). For the first time the wurtzite-like ($\beta\text{-Ga}_2\text{S}_3$, $P6_3mc$) and sphalerite-like ($\gamma\text{-Ga}_{2+\delta}\text{S}_3$) defect structures (with disordered vacancies) were obtained under equilibrium and studied *in situ* by means of synchrotron radiation.

For the first time a phase diagram of the Ga – S system was obtained and the regions of existence of the three above listed high-temperature gallium sesquisulfides and a modification of gallium sesquisulfide ($\alpha'\text{-Ga}_2\text{S}_3$, Cc), stable at room temperature, were determined.

Contribution of the authors

At the end of the Conclusions the authors should include notes that explain the actual contribution of each co-author to the work.

Conflict of interests

The authors declare that they have no known competing financial interests or personal relationships that could have influenced the work reported in this paper.

References

1. Dingqi T., Haiyun L., Yuan D., Zhengliang D., Jiaolin C. Engineered cation vacancy plane responsible for the reduction in lattice thermal conductivity and

improvement in thermoelectric property of Ga_2Te_3 based semiconductors. *RSC Advances*. 2014;4: 34104–34109. <https://doi.org/10.1039/c4ra04463k>

2. Fedorov P. P., Yarotskaya E. G. Zirconium dioxide. Review. *Condensed Matter and Interphases*. 2021;23(2): 169–187. <https://doi.org/10.17308/kcmf.2021.23/3427>

3. Budanov A. V., Tatokhin E. A., Strygin V. D., Rudnev E. V. High-symmetry in In_2Se_3 and Ga_2Se_3 cubic modifications obtained during interaction of InAs and GaAs substrates and selenium. *Condensed Matter and Interphases*. 2012;14(4): 412–417. (In Russ., abstract in Eng.). Available at: <https://www.elibrary.ru/item.asp?id=18485334>

4. Bezryadin N. N., Kotov G. I., Kuzuhov S. V. ... Ryazanov A. N. Surface phase Ga_2Se_3 на GaP (111). *Condensed Matter and Interphases*. 2013;15(4): 382–386. (In Russ., abstract in Eng.). Available at: <https://www.elibrary.ru/item.asp?id=20931229>

5. Mikhailyuk E. A., Prokopova T. V., Bezryadin N. N. Modeling of processes of current flow films $\text{A}^{\text{III}}_2\text{B}^{\text{VI}}_3$ in heterostructures on the basis of indium arsenide. *Condensed Matter and Interphases*. 2015; 17(2): 181–191. (In Russ., abstract in Eng.). Available at: <https://www.elibrary.ru/item.asp?id=23816619>

6. Plirdpring T., Kurosaki K., Kosuga A., ... Yamanaka S. Effect of the amount of vacancies on the thermoelectric properties of CuGaTe ternary compounds. *Materials Transactions (Special Issue on Thermoelectric Conversion Materials VII)*. 2012;53(7): 1212–1215. <https://doi.org/10.2320/matertrans.e-m2012810>

7. Olmstead M. A., Ohuchi F. S. Group III selenides: Controlling dimensionality, structure, and properties through defects and heteroepitaxial growth. *Journal of Vacuum Science & Technology A: Vacuum, Surfaces, and Films*. 2021;39(2): 020801. <https://doi.org/10.1116/6.0000598>

8. Zavrazhnov A., Berezin S., Kosykov A., Naumov A., Berezina M., Brezhnev N. The phase diagram of the Ga–S system in the concentration range of 48.0–60.7 mol% S. *Journal of Thermal Analysis and Calorimetry*. 2018;134: 483–492. <https://doi.org/10.1007/s10973-018-7124-z>

9. Volkov V. V., Sidey V. I., Naumov A. V., ... Zavrazhnov A. Y. The cubic high-temperature modification of gallium sulphide ($x_s = 59$ mol %) and the *T, x*-diagram of the Ga – S system. *Condensed Matter and Interphases*. 2019;21(1): 37–50. (In Russ., abstract in Eng.). <https://doi.org/10.17308/kcmf.2019.21/715>

10. Volkov V. V., Sidey V. I., Naumov A. V., ... Zavrazhnov A. Yu. Structural identification and stabilization of the new high-temperature phases in A(III) – B(VI) systems (A = Ga, In, B = S, Se). Part 1: High-temperature phases in the Ga – S system. *Journal*

of *Alloys and Compounds*. 2022;899: 163264. <https://doi.org/10.1016/j.jallcom.2021.163264>

11. Pardo M., Tomas A., Guittard M. Polymorphisme de Ga₂S₃ et diagramme de phase Ga – S. *Materials Research Bulletin*. 1987;22(12): 1677–1684. [https://doi.org/10.1016/0025-5408\(87\)90011-0](https://doi.org/10.1016/0025-5408(87)90011-0)

12. Pardo M., Guittard M., Chilouet A., Tomas A. Diagramme de phases gallium-soufre et études structurales des phases solides. *Journal of Solid State Chemistry*. 1993;102: 423–433. <https://doi.org/10.1006/jssc.1993.1054>

13. Sushkova T. P., Semenova G. V., Proskurina E. Y. Phase relations in the Si–Sn–As system. *Condensed Matter and Interphases*. 2023;25(2), 237–248. <https://doi.org/10.17308/kcmf.2023.25/11110>

14. Kraus W., Nolze G. PowderCell 2.0 for Windows. *Powder Diffraction*. 1998;13(4): 256–259. Available at: https://www.researchgate.net/publication/257022604_PowderCell_20_for_Windows

15. Hammersley A. P., Svensson S. O., Hanfland M., Fitch A. N., Hausermann D. Two-dimensional detector software: From real detector to idealised image or two-theta scan. *High Pressure Research*. 1996;14(4–6): 235–248. <https://doi.org/10.1080/08957959608201408>

16. Holland T. J. B., Redfern S. A. T. UNITCELL: a nonlinear least-squares program for cell-parameter refinement and implementing regression and deletion diagnostics. *Journal of Applied Crystallography*. 1997;30(1): 84. <https://doi.org/10.1107/s0021889896011673>

17. Fedorov P. I., Fedorov P. P., Drobot D. V., Samartsev A. M. *Errors in constructing state diagrams of binary systems: a textbook**. Moscow: MITHT named after M. V. Lomonosova Publ.; 2005. 181 p. (In Russ.)

18. Parthé E. *Elements of inorganic structural chemistry*. CH-1213: Petit-Lancy, Switzerland; 1996. 230 p.

19. Sangiovanni D. G., Kaufmann K., Vecchio K. Valence electron concentration as key parameter to control the fracture resistance of refractory high-entropy carbides. *Science Advances*. 2023;9(37): 1–11. <https://doi.org/10.1126/sciadv.adi2960>

20. Gilbert B., Frazer B. H., Zhang H., ... De Stasio G. X-ray absorption spectroscopy of the cubic and hexagonal polytypes of zinc sulfide. *Physical Review B*. 2002;66: 245205. <https://doi.org/10.1103/physrevb.66.245205>

Information about the authors

Nikolay Y. Brezhnev, Junior Researcher at the Department of General and Inorganic Chemistry, Voronezh State University (Voronezh, Russian Federation).

<https://orcid.org/0000-0002-3287-8614>
brezhnevnick@gmail.com

Michael V. Dorokhin, Dr. Sci (Phys.-Math.), Leading Researcher at the Physical-Technical Research Institute of UNN (PTRI) (Nizhny Novgorod, Russian Federation).

<https://orcid.org/0000-0001-5238-0090>
dorokhin@nifti.unn.ru

Alexander Y. Zavrazhnov, Dr. Sci. (Chem.), Full Professor, Department of General and Inorganic Chemistry, Voronezh State University (Voronezh, Russian Federation).

<https://orcid.org/0000-0003-0241-834X>
alexander.zavrazhnov@gmail.com

Nikolay A. Kolyshkin, Research Engineer at the National Research Center “Kurchatov Institute” (Moscow, Russian Federation).

<https://orcid.org/0000-0003-3437-6391>
nickelprog@mail.ru

Ivan N. Nekrylov, post-graduate student at the Department of General and Inorganic Chemistry, Voronezh State University (Voronezh, Russian Federation).

<https://orcid.org/0000-0003-4491-4739>
Icq492164858@gmail.com

Vladimir N. Trushin, Dr. Sci (Phys.-Math.), Leading Researcher at the Physical-Technical Research Institute of UNN (PTRI) (Nizhny Novgorod, Russian Federation).

<https://orcid.org/0000-0001-5104-6592>
trushin@phys.unn.ru

Received 08.09.2023; approved after reviewing 02.10.2023; accepted for publication 15.11.2023; published online 25.06.2024.

Translated by Yulia Dymant